

# PHYSICAL REVIEW LETTERS

VOLUME 54

27 MAY 1985

NUMBER 21

## Delocalization Transition of a Classical Two-Dimensional Coulomb Lattice

Jean Clerouin and Jean-Pierre Hansen<sup>(a)</sup>

*Commissariat à l'Energie Atomique, F-94190 Villeneuve/St. Georges, France*

(Received 28 January 1985)

The dielectric-plasma transition of the two-dimensional Coulomb gas, suitably mapped onto a delocalization transition, is investigated by molecular-dynamics simulations. The threshold temperature  $T_1$  for electrical conduction falls well below the temperature  $T_2$  associated with a marked peak in the specific heat;  $T_2$  is close to the mean-field prediction for the Kosterlitz-Thouless transition,  $k_B T_2/e^2 = \frac{1}{4}$ .

PACS numbers: 05.60.+w, 52.25.Kn, 61.20.Ja

The symmetric two-dimensional Coulomb gas, consisting of equal numbers of oppositely charged particles which interact through the logarithmic Coulomb potential  $\pm e^2 \ln(r/L)$  (where  $e$  is the electric charge and  $L$  an arbitrary length scale), is known to be thermodynamically stable for reduced temperatures  $T^* = k_B T/e^2$  above  $\frac{1}{2}$ .<sup>1</sup> Below that temperature a short-range cutoff (for  $r < \sigma$ ) of the Coulomb attraction is needed to prevent the collapse of pairs of oppositely charged particles. A mean-field argument shows that this system will undergo a transition from a conducting plasma phase to an insulating dielectric phase, occurring at  $T^* = \frac{1}{4}$  in the low-density limit where  $\sigma$  is much less than the mean interparticle spacing.<sup>2,3</sup> In this Letter we report results of "molecular-dynamics" simulations of a Kosterlitz-Thouless (KT) transition in a related dissymmetric Coulomb model with one charged species fixed on a triangular lattice.

Our model consists of  $N$  positive "ions" and  $N$  negative "electrons" interacting through the pair potential:

$$v_{\alpha\beta}(r) = e^2 [(\sigma_{\alpha\beta}/r)^\nu - Z_\alpha Z_\beta \ln(r/L)], \quad (1)$$

where  $1 \leq \alpha, \beta \leq 2$  are species indices;  $Z_\alpha, Z_\beta = \pm 1$ ;  $\sigma_{11} = \sigma_{22} = 0$ ;  $\sigma_{12} = \sigma > 0$ ; and the exponent of the short-range ion-electron repulsion is chosen to be  $\nu = 10$ . The ions (of infinite mass) are fixed on the sites of a hexagonal lattice, while the  $N$  interacting electrons (of mass  $m$ ) move in the periodic field of the ions so that our model could also be interpreted as a

one-component plasma of classical electrons in a periodic (rather than uniform) neutralizing ionic field. In this way we have mapped the KT plasma-dielectric transition onto an equivalent classical localization transition. Restricting the ions to a lattice simplifies the simulations and allows us to bypass a possible first-order transition from a low-density "gas" phase to a high-density "liquid" phase, as observed in three-dimensional electrolytes.<sup>4</sup> The choice  $\sigma_{11} = \sigma_{22} = 0$  is not an important restriction because of the Coulomb repulsion between like particles and because ions are fixed on a lattice.

A thermodynamic state of the model is characterized by  $T^*$  (or  $\gamma = 1/T^*$ ) and the ratio of  $\sigma$  over the "ion-disk" radius  $a = (\pi n)^{-1/2}$ , where  $n = N/S$  is the number of ions (or electrons) per unit area; all the simulations reported here have been carried out for  $\sigma/a = 0.1$ , but preliminary calculations with  $\sigma/a = 0.2$  indicate qualitatively similar behavior.

The simulation cell was chosen to be a hexagon containing  $N = 75, 108, \text{ or } 192$  ions and as many electrons, with periodic boundary conditions. The long-range Coulomb forces were effectively truncated by adoption of the standard nearest-image convention. This time-saving procedure is certainly justified in the low-temperature limit, where ions and electrons form tightly bound neutral pairs. In the high-temperature plasma phase a more satisfactory (but time-consuming) procedure would be to perform Ewald summations of the Coulomb forces over all periodic im-

ages,<sup>5</sup> but experience gained from simulations of three-dimensional electrolytes<sup>6</sup> indicates that the simpler nearest-image convention should be adequate at intermediate coupling ( $\gamma \approx 1$ ). The coupled equations of motion of the  $N$  electrons were numerically integrated by the standard Verlet finite-difference algorithm.<sup>7</sup> The choice of time step is dictated by the characteristic frequencies of the system. In the high-temperature plasma phase ( $T^* > \frac{1}{4}$ ) we expect the dynamics to be dominated by the collective electron plasma frequency  $\omega_p = (2\pi ne^2/m)^{1/2}$ , while in the low-temperature dielectric phase the characteristic frequencies are those of the individual motion of each electron in the field of the ion with which it is paired. Let  $r$  and  $\theta$  denote the polar coordinates of an electron with respect to its partner ion. If we neglect interaction between pairs, an elementary calculation of the mean square angular velocity valid in the limit where  $\gamma \rightarrow \infty$  in Eq. (1) yields the following estimate of the characteristic frequency  $\omega_r$  associated with the rotational motion:

$$\omega_r = [\langle \dot{\theta}^2 \rangle]^{1/2} = \left( \frac{e^2}{m\sigma^2} \right)^{1/2} \frac{(\gamma-2)^{1/2}}{\gamma}, \quad \gamma > 2. \quad (2)$$

The ratio  $\omega_r/\omega_p$  vanishes in the limits  $\gamma \rightarrow \infty$  and  $\gamma \rightarrow 2^+$ , and takes its maximum value 2.5 for  $\gamma=4$ . The characteristic vibrational frequency  $\omega_v$  associated with the radial motion is most conveniently estimated from the Einstein frequency occurring in the short-time expansion of the normalized electron velocity autocorrelation function<sup>8</sup>  $Z(t)$ :

$$Z(t) = \langle \mathbf{v}(t) \cdot \mathbf{v}(0) \rangle / \langle v^2 \rangle \quad (3a)$$

$$= 1 - (\omega_v^2/2!)t^2 + O(t^4), \quad (3b)$$

$$\omega_v^2 = 2m^{-1} \langle \nabla^2 \Phi \rangle, \quad (3c)$$

where  $\Phi$  denotes the total potential acting on an electron. Retaining only the contribution of the nearest ion we find

$$\omega_v = \nu^{1/2} \left( \frac{e^2}{m\sigma^2} \right)^{1/2} \left[ \frac{(\gamma-2)}{\gamma^{1+2/\nu}} \frac{\Gamma(1+\gamma/\nu)}{\Gamma(1+(\gamma-2)/\nu)} \right]^{1/2}. \quad (4)$$

With  $\nu=10$ ,  $\omega_v/\omega_p \approx 10$  for  $\gamma \geq 4$ , and vanishes as  $\gamma \rightarrow 2^+$ . Because of the presence of this relatively high vibrational frequency, we have chosen a sufficiently short time step,  $\Delta t \approx 0.005$ , in our simulations to ensure a good conservation of the total energy. In order to achieve sufficient statistical accuracy, runs of total length comprised between  $10^2\omega_p^{-1}$  and  $10^3\omega_p^{-1}$ , after initial equilibration, were carried out. The simulations covered the range  $15 \geq \gamma \geq 1$ , with particular emphasis on the vicinity of  $\gamma=4$  where the KT transition is expected to take place. The salient results can

be summarized as follows.

(1) The complete trajectories of all electrons were monitored for each  $\gamma$  and displayed graphically. As expected, these trajectories are strongly localized for low temperatures ( $\gamma > 6$ ); delocalization of the electrons occurs gradually for  $\gamma \leq 6$ . At first (for  $6 \geq \gamma \geq 4$ ) tightly bound ion-electron pairs are observed to coexist with delocalized electrons which appear to be exchanged between ions (see Fig. 1). For still higher temperatures ( $\gamma \leq 4$ ) the electronic trajectories become more and more space filling. In summary, the observed KT transition appears to be very gradual, with the coexistence of localized and delocalized electron states persisting over a certain range of temperatures.

(2) At the lowest temperatures ( $\gamma \geq 10$ ), when each electron is tightly bound to its ionic partner, the question naturally arises whether the system thermalizes over time intervals sufficiently short compared to the total length of the runs. We have checked that the velocity distribution of the electrons tends rapidly towards a Maxwellian even at the lowest temperatures, independently of the initial conditions; thus the residual dipolar interactions between tightly bound pairs is sufficient to ensure thermalization over a reasonable number of time steps.

(3) We have investigated a certain number of static and dynamic diagnostics for a quantitative characterization of the KT transition. The most obvious diagnostic is the onset of diffusion. We have computed the electron velocity autocorrelation function  $Z(t)$ , defined in Eq. (3a), and its Fourier transform (or spectral function)  $\hat{Z}(\omega)$ . At temperatures well below

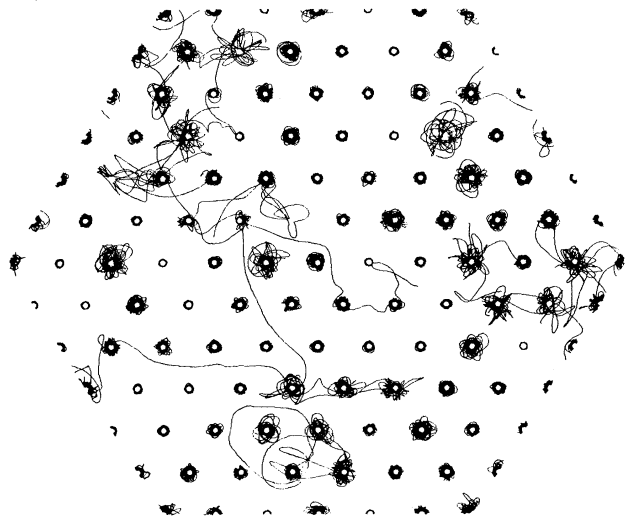


FIG. 1. Trajectories of 108 electrons for  $\gamma=4.3$ ,  $\sigma=0.1$ , integrated over  $300\omega_p^{-1}$ . Ions are fixed on a triangular lattice.

the KT transition,  $Z(t)$  exhibits a fast initial decay and pronounced oscillations; the spectral analysis reveals a relatively sharp peak at a frequency compatible with the rotational frequency  $\omega_r$ , defined in Eq. (2), as well as a broad band at much higher frequencies ( $\geq 10\omega_p$ ), corresponding to the vibrational motion of Eq. (4). As the temperature increases, the vibrational band reduces to a continuum decaying slowly at high frequencies; the rotational peak broadens more gradually, shifts first to higher frequencies (for  $\gamma \geq 6$ ), then to lower frequencies as the temperature rises, in agreement with the estimate of Eq. (2). Below  $\gamma \approx 4$  the rotational peak moves rapidly towards zero frequency, and for  $\gamma \leq 2$  the spectrum  $\hat{Z}(\omega)$  reduces to a Lorentzian-type central peak. Two typical examples corresponding to  $\gamma = 5.7$  (dielectric phase) and  $\gamma = 1.8$  (plasma phase) are shown in Figs. 2(a) and 2(b). The electronic self-diffusion constant  $D$  is directly proportional to the time integral of  $Z(t)$ , i.e., to  $\hat{Z}(\omega=0)$ ; the variation of  $D^* = D/\omega_p a^2$  with temperature is shown in Fig. 3.  $D^*$  is seen to vanish somewhere in the range  $6 \geq \gamma \geq 5.5$ , but the statistical uncertainties are at present too large to allow a more accurate determination of the threshold temperature  $T_1^*$  and the pre-

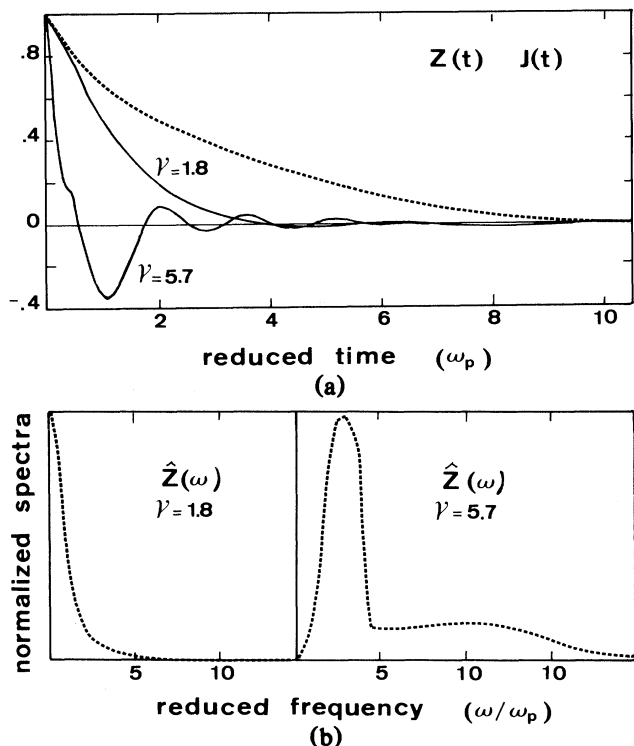


FIG. 2. (a) Normalized velocity and current autocorrelation functions  $Z(t)$  and  $J(t)$  vs reduced time for  $\gamma = 5.7$  and  $\gamma = 1.8$ . Solid curves,  $Z(t)$ ; dotted curves,  $J(t)$  at  $\gamma = 1.8$ . (b) Normalized spectra  $\hat{Z}(\omega)$  for  $\gamma = 5.7$  and  $\gamma = 1.8$  vs reduced frequency.

cise law according to which  $D$  vanishes with  $T^* - T_1^*$ .

(4) The electrical conductivity is similarly given by the time integral of the electric current autocorrelation function<sup>8</sup>  $J(t)$ :

$$J(t) = \frac{m}{2Nk_B T} \left\langle \sum_i \mathbf{v}_i(t) \cdot \sum_\gamma \mathbf{v}_\gamma(0) \right\rangle. \quad (5)$$

Since  $J(t)$  is a collective property, its molecular-dynamics estimates are subject to much larger statistical uncertainties than  $Z(t)$ . Nevertheless, our data give strong indications that  $J(t)$  is practically indistinguishable from  $Z(t)$  for  $\gamma \geq 4$  (i.e., essentially in the dielectric phase), as would be expected if cross correlations between the velocities of different electrons were negligible in Eq. (5). Under these conditions  $\sigma^* = \sigma/\omega_p = (\gamma/\pi)D$  so that the conductivity vanishes with the diffusion constant, as expected.

On the other hand, when  $\gamma \leq 4$  (i.e., in the plasma phase), the difference between  $J(t)$  and  $Z(t)$  increases rapidly, the electric current decaying more and more slowly compared to the electron velocity, as illustrated in Fig. 2(a). This effect has already been observed in simulations of strongly coupled ion-electron plasmas in three dimensions<sup>9</sup> and can be ascribed to the fact that electron-electron collisions decorrelate the individual velocities, but not the total electric current, because of momentum conservation. Under these conditions  $\sigma^*$  is significantly larger (by a factor of 2.2 at  $\gamma = 1.8$ ) than its Nernst-Einstein estimate  $(\gamma/\pi)D$ .

(5) The reduced excess internal energy per electron,  $U = \langle V \rangle / Ne^2$ , is plotted as a function of temperature in Fig. 3.  $U(T^*)$  is seen to be linear at low tempera-

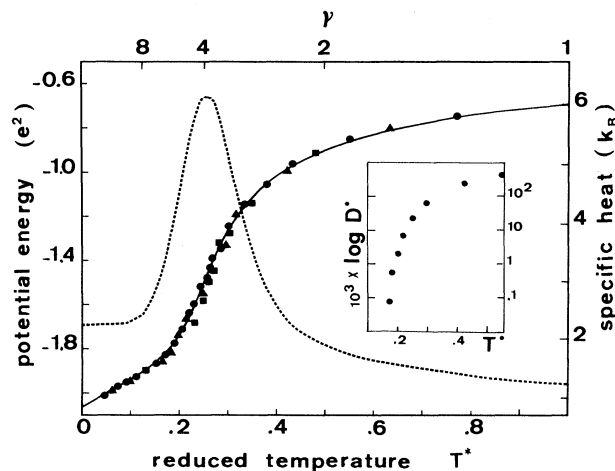


FIG. 3. Excess internal (potential) energy per electron (circles are simulation results for  $N = 108$ ; squares,  $N = 75$ ; and triangles,  $N = 192$ ; the solid curve is our best fit) and total specific heat  $C$  per electron (deduced from best fit) vs reduced temperature. Inset: the logarithm of the reduced diffusion constant vs temperature.

tures, to increase rapidly in the range  $0.2 \leq T^* \leq 0.3$ , and then to saturate at higher temperatures. The simulation results for the energy exhibit no visible  $N$  dependence. The simulation data are reasonably well fitted (within better than 2% at all temperatures) by the function

$$U(T^*) = \frac{a_0 + a_1 T^* + a_2 T^{*2} + a_3 T^{*3}}{1 + a_4 T^* + a_5 T^{*2} + a_6 T^{*3}}, \quad (6)$$

with

$$a_0 = -2.0642, \quad a_1 = 9.4218, \quad a_2 = -16.3848,$$

$$a_3 = 3.3972, \quad a_4 = -3.9203, \quad a_5 = 3.5851,$$

$$a_6 = 17.4697,$$

corresponding to the choice  $L = a$  for the arbitrary scaling length of the Coulomb potential in Eq. (1). The zero-temperature limit  $a_0$  of  $U$  lies slightly below the corresponding limit for a single ion-electron pair, i.e.,  $U_0 = \ln(\sigma/a) + (1 + \ln\gamma)/\gamma = -1.9723$ , this fact stressing again the importance of residual dipolar interactions between pairs which are responsible for the good thermalization of our model system. The specific heat (per electron) at constant area,  $C$ , is obtained by differentiation of  $U(T^*)$  with respect to  $T^*$ .  $C$  is found to go through a relatively broad maximum at a temperature  $T^* \approx 0.26$  before decaying to zero at high temperatures. The peak in the specific heat occurs thus at a temperature close to the Kosterlitz-Thouless mean-field prediction,<sup>2</sup> but it is important to realize that this is well above the delocalization threshold temperature which our simulations have shown to be less than 0.2. On the other hand, the preliminary simulations for a ratio  $\sigma/a = 0.2$  indicate that both the delocalization threshold and the specific-heat maximum are shifted to lower temperatures ( $\gamma \approx 8$  and 7, respectively).

Thus the dielectric-plasma transition is seen to take place in two steps. First, at a threshold temperature  $T_1$ , delocalization sets in, as signaled by a nonzero value of the self-diffusion coefficient of the electrons. Above  $T_1$  the system is a conductor, so that the dielectric constant is expected to diverge at  $T_1$ . Just above  $T_1$ , electrical conduction is essentially a "hopping"

process, which means that ion-electron pairs have a temperature-dependent finite lifetime. The delocalization threshold is hence essentially dynamical in nature and does not appear to have any thermodynamic implications. At a temperature  $T_2 > T_1$  the specific heat exhibits a peak which can be associated with the final breakup of the pairs, when the "chemical equilibrium" between "bound" and "free" electrons is broken in favor of the latter "species." In other words, for  $T \geq T_2$ , the mean lifetime of an ion-electron pair becomes of the order of the spacing between ions ( $a$ ) divided by the thermal electron velocity  $[(k_B T/m)^{1/2}]$ . The distinction between  $T_1$  and  $T_2$  is somewhat reminiscent of the appearance of the "premelting" phenomena observed, e.g., in simulations of the melting transition of the two-dimensional one-component plasma.<sup>10</sup>

We are presently investigating the density dependence of our results more systematically by varying the ratio  $\sigma/a$ . We are also planning to investigate the influence of disorder on the KT transition by "melting" the ion lattice, which leads to a symmetric Coulomb gas.

<sup>(a)</sup>Permanent address: Ecole Normale Supérieure de Saint Cloud, F-92210 Saint Cloud Cedex, France.

<sup>1</sup>E. H. Hauge and P. C. Hemmer, *Phys. Norv.* **5**, 209 (1971).

<sup>2</sup>J. M. Kosterlitz and D. J. Thouless, *J. Phys. C* **6**, 1181 (1973).

<sup>3</sup>J. Fröhlich and T. Spencer, *Phys. Rev. Lett.* **46**, 1006 (1981).

<sup>4</sup>H. L. Friedman and B. Hafskjold, *J. Chem. Phys.* **70**, 92 (1979).

<sup>5</sup>J. W. Perram and S. W. de Leeuw, *Physica (Utrecht)* **109A**, 237 (1981).

<sup>6</sup>D. J. Adams, *Chem. Phys. Lett.* **62**, 239 (1979).

<sup>7</sup>L. Verlet, *Phys. Rev.* **159**, 98 (1967).

<sup>8</sup>J. P. Hansen and I. R. McDonald, *Theory of Simple Liquids* (Academic, London, 1976).

<sup>9</sup>J. P. Hansen and I. R. McDonald, *Phys. Rev. A* **23**, 2041 (1981); L. Sjögren, J. P. Hansen, and E. L. Pollock, *Phys. Rev. A* **24**, 1544 (1981).

<sup>10</sup>Ph. Choquard and J. Clerouin, *Phys. Rev. Lett.* **50**, 2086 (1983).